Phys. Status Solidi B **250**, No. 2, 329–333 (2013) / **DOI** 10.1002/pssb.201248374

physica status solidi b
www.pss-b.com
basic solid state physics

Raman-scattering probe of anharmonic effects due to temperature and composition in InGaN

J. F. Kong[*,1], **W. Z. Shen**[2], **and Q. X. Guo**[3]

[1] School of Science, Shanghai Institute of Technology, 100 Hai Quan Road, Shanghai 201418, P. R. China
[2] Laboratory of Condensed Matter Spectroscopy and Opto-Electronic Physics, Key Laboratory of Artificial Structures and Quantum Control (Ministry of Education), Department of Physics, Shanghai Jiao Tong University, 800 Dong Chuan Road, Shanghai 200240, P. R. China
[3] Synchrotron Light Application Center, Department of Electrical and Electronic Engineering, Saga University, Saga 840-8502, Japan

Received 13 August 2012, revised 23 October 2012, accepted 6 November 2012
Published online 5 December 2012

Keywords nitride semiconductors, phonons, Raman scattering, thin films

[*] Corresponding author: e-mail jfkong@sit.edu.cn, Phone: 86-21-60873193, Fax: 86-21-60873193

We have carried out a detailed investigation of temperature-dependent micro-Raman scattering on $In_{1-x}Ga_xN$ films with different Ga compositions ($0.06 \leq \chi \leq 0.91$). The observed phonon frequency downshift and linewidth broadening with increasing temperature of A_1(LO) and E_2(high) modes can be well explained by a model taking into account the contributions of the thermal expansion, the lattice-mismatch-induced strain, and the anharmonic phonon processes. We have elucidated the variation with Ga composition of the contribution of the three- and four-phonon processes in the anharmonic effect. It is found that with increasing Ga composition the three-phonon process increases over the four-phonon process. The variation in the relative contribution from three- and four-processes can be further attributed to the diversification of structural properties and phonon density of states in InGaN.

© 2012 WILEY-VCH Verlag GmbH & Co. KGaA, Weinheim

1 Introduction Considerable attention has been recently paid to $In_{1-x}Ga_xN$ materials for its promising application for light-emitting diodes, laser diodes, photo-detectors, high-power and high-speed electronic devices, and solar cell [1–5], since they offer a possibility of tuning band gap from near-IR to ultraviolet regimes. There have been numerous reports about the growth of $In_{1-x}Ga_xN$ by a variety of methods [5–9]. However, growth of $In_{1-x}Ga_xN$ alloys has been very difficult due to solid miscibility gap or phase separation induced by large difference in interatomic spacing between InN and GaN, which strongly affect the optical properties of the InGaN layers. Given the numerous applications of InGaN semiconductors in optical devices, it is important to clearly understand the structural and optical properties of these materials. In particular, the phonon modes play a dominant role in the electron scattering processes.

Raman scattering, as a fast, nondestructive, and contactless technique, can directly probe the lattice vibration of semiconductors which strongly affect the band structure and behavior of carriers. Therefore, Raman spectroscopy has been widely employed in InGaN at room temperature [9–15]. Changes of the frequency and linewith of Raman mode with temperature can further provide basic information of the lattice dynamics. Furthermore, the information of phonon decay is an essential aspect to understand the phonon behaviors. In contrast to the comprehensive investigation of temperature effect of Raman scattering for other semiconductors, *e.g.*, GaN, InN, and ternary alloys [16–19], there is no detailed temperature dependence of phonon behavior in InGaN. The introduction of Ga in InN will result in the modifications of the crystal lattice, which may breakdown the translational symmetry. What is the phonon decay characteristic in InGaN and how is the decay process related with the Ga concentration are still open questions.

In this paper, we have presented a comprehensive investigation of temperature-dependent Raman spectra of A_1(longitudinal optical (LO)) and E_2(high) modes in hexagonal InGaN films with different Ga compositions (0.06–0.91) grown by reactive radio-frequency magnetron sputtering in the temperature range from 83 to 443 K.

© 2012 WILEY-VCH Verlag GmbH & Co. KGaA, Weinheim

Through detailed theoretical modelings for the frequencies downshift and linewidths broadening, we have clearly illustrated the temperature effect on the phonon frequency and linewidth in the ternary InGaN thin films.

2 Experimental details InGaN films were prepared on (0001) sapphire substrates by reactive radio-frequency magnetron sputtering in nitrogen plasma. Double-side-polished (0001) sapphire substrates were cleaned ultrasonically in organic solvents, chemically etched in a hot H_3PO_4:H_2SO_4 (1:3) solution, and rinsed in deionized water. The sputtering chamber was evacuated to a pressure of 10–7 Torr using a turbomolecular pump before introducing the nitrogen gas. During the growth, the gas flow rate, sputter power, and pressure were maintained at 4 sccm, 100 W, and 5 mTorr, respectively. The substrate temperature was monitored using a thermocouple and controlled at a given value between 100 and 550 °C. It was found that In, Ga, As, and N atoms absorb on the substrate and react with each other to form an InGaNAs film at a low substrate temperature. With increasing the substrate temperature to 550 °C, the arsenic atom in the grown layer are completely desorbed, forming the InGaN film. A GaAs wafer was mounted on the indium target and the area ratio of the GaAs wafer to the indium target was varied to obtain InGaN films with the desired composition. Chemical compositions of the obtained films were measured by energy-dispersive X-ray spectroscopy. Temperature-dependent micro-Raman scattering spectra from 83 to 443 K were recorded in a backscattering geometry of $z(x,-)\bar{z}$ configuration using a Jobin Yvon LabRAM HR 800UV system under the 514.5 nm line of an Ar-ion laser. The employment of a 50× optical microscopy objective with a numerical aperture of 0.5 will yield a laser spot size of ~1.3 μm.

3 Results and discussion Figure 1(a) displays the typical temperature-dependent micro-Raman spectra of $In_{0.83}Ga_{0.17}N$ with the error bars, where the contributions of the InGaN emission have been subtracted from the measured Raman spectra by using baselines in the relevant software of the micro-Raman system. It can be seen that the dominant peak shifts to lower frequency and broadens with the increase of temperature. In order to identify each part of the contribution, we have fitted the observed Raman spectra with Lorentz peaks. Figure 1(b) shows the detailed analysis of the Raman spectrum for $In_{0.83}Ga_{0.17}N$ at 83 K (circles) with two peaks a and b at about 526 and 598 cm^{-1}, respectively. According to the selection rules, the E_2(high) and A_1(LO) modes are activated for wurtzite crystalline InGaN in the measured Raman geometry configuration [5, 20]. Thus, we have assigned the modes at ~526 and 598 cm^{-1} to the E_2(high) and A_1(LO) phonon modes of InGaN, respectively, with a full width at half maximum of the A_1(LO) peak ~100 cm^{-1}, which indicate the relatively low crystalline quality of the present hexagonal $In_{1-x}Ga_xN$ samples compared with that of A_1(LO) peak (~75 cm^{-1}) grown by epitaxial methods [21]. The above Lorentz fitting

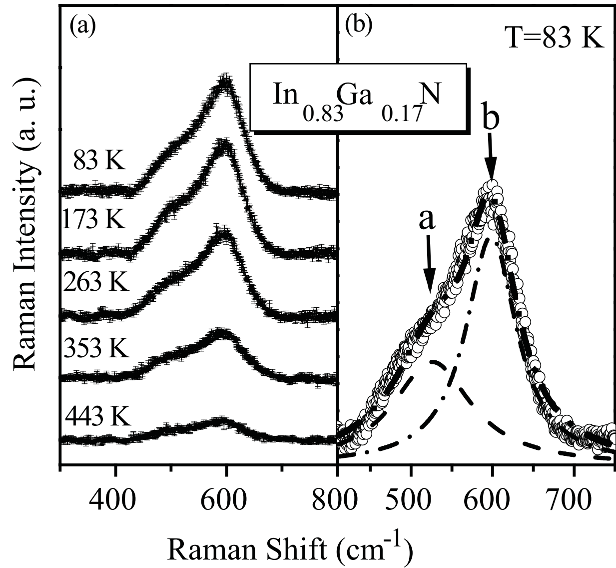

Figure 1 (a) Temperature-dependent Raman spectra of $In_{0.83}Ga_{0.17}N$ with the error bars and (b) Raman spectrum from $In_{0.83}Ga_{0.17}N$ at 83 K, where the solid curve is the fitting results using three Lorentz peaks (dashed curves) with (a) E_2(high) and (b) A_1(LO).

processes are employed to obtain the detailed temperature and Ga-composition dependences of the phonon frequency and linewidth. In the following, we concentrate on the phonon characteristics of the E_2(high) and A_1(LO) modes in the $In_{1-x}Ga_xN$ alloy.

Figure 2 illustrates the frequencies of the A_1(LO) and E_2(high) modes with temperature. The downshift of the Raman frequency with the increase of temperature is mainly due to the effects of thermal expansion, lattice-mismatch-induced strain, and anharmonic coupling to other phonons. In modeling the Raman shift, we can write the temperature-dependent Raman frequency $\omega(T)$ as [16–18]

$$\omega(T) = \omega_0 + \Delta\omega_e(T) + \Delta\omega_s(T) + \Delta\omega_d(T), \quad (1)$$

where ω_0 is the harmonic frequency, $\Delta\omega_e(T)$ the contribution of thermal expansion or volume change, $\Delta\omega_s(T)$ the lattice and thermal mismatch between the InGaN thin films and sapphire substrate, and $\Delta\omega_d(T)$ is the one due to the anharmonic coupling to phonons of other branches. The term $\Delta\omega_e(T)$ can be given by $\Delta\omega_e(T) = -\omega_0\gamma\int_0^T[\alpha_c(T') + 2\alpha_a(T')]dT'$, where γ is the Grüneisen parameter for the optical Raman mode [17, 18], α_c and α_a are the parallel and perpendicular temperature-dependent coefficients of linear thermal expansion, respectively [17, 22]. The strain-induced term $\Delta\omega_s(T)$ can be written as $\Delta\omega_s(T) = [2a - (2C_{13}/C_{33})b]\varepsilon(T)$, where $\varepsilon(T)$ is a temperature dependence of in-plane strain for the different thermal expansion coefficients between thin film and substrate [17]. The phonon deformation potentials a and b, as well as the elastic constants C_{13} and C_{33}, are taken from Refs. [16] and [17].

© 2012 WILEY-VCH Verlag GmbH & Co. KGaA, Weinheim

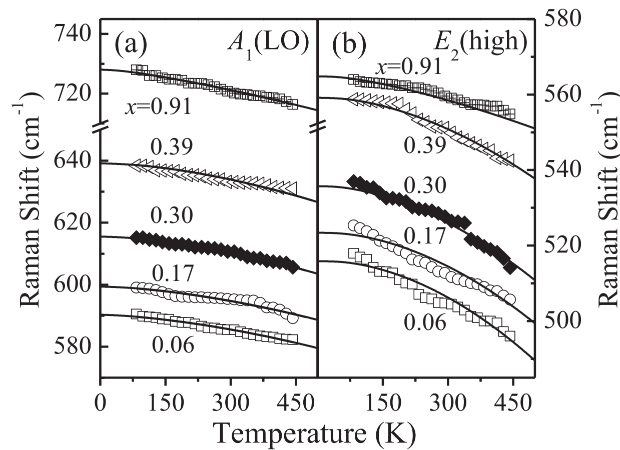

Figure 2 Temperature-dependent Raman frequencies of (a) A_1(LO) and (b) E_2(high) modes in InGaN with different Ga compositions. The solid curves are the theoretical calculation results with Eqs. (1) and (2).

For the anharmonic coupling term $\Delta\omega_d(T)$, we can model it by taking into account cubic and quartic terms in anharmonic Hamiltonian [16–18]:

$$\Delta\omega_d(T) = M_1[1 + n(T, \omega_1) + n(T, \omega_2)] + M_2\left[1 + 3n(T, \omega_0/3) + 3n^2(T, \omega_0/3)\right], \quad (2)$$

with M_1 and M_2 being constants, which are selected as fitting parameters in the calculation, and $n(T, \omega) = [\exp(\hbar\omega/k_B T) - 1]^{-1}$ the Bose–Einstein function. The first term corresponds to the decay into two phonons of frequency ω_1 and ω_2 (three-phonon process), with $\omega_1 + \omega_2 = \omega_0$; while the second term represents the decay into three phonons (four-phonon process), and energy conservation can be satisfied in the simple Klemens fashion by setting $\omega = \omega_0/3$ [23, 24]. However, in the case of InN, the zone-center LO phonons cannot decay into two longitudinal acoustic (LA) or transverse-acoustic (TA) phonons of equal frequencies and opposite wave vectors due to the large energy gap between the acoustic and optical phonon branched in InN $\omega_{LO} > 2\omega_{LA,TA}$ [17]; whereas, it is possible to decay into a large wave-vector transverse optical (TO) and a large wave-vector LA or TA phonon. On the other hand, the E_2(high) phonons cannot decay into either two LA (TA) phonons [the energy gap between the acoustic- and the optical-phonon branches is more than one half of the E_2(high) phonon energy] or one TO and one LA (TA) phonons [E_2(high) is at the lower edge of the optical-phonon branch]. As a result, only the four-phonon process has been taken into account in the decay of the E_2(high) phonon in InN. However, the energy gap of $In_{1-x}Ga_xN$ shifts toward higher energies with the increasing of Ga composition, leading to an increase of the probability the three-phonon process. Therefore, we have employed the similar decay processes for the temperature dependence of Raman frequencies of A_1(LO) mode, and the symmetric decay for the temperature dependence of Raman frequencies of E_2(high) mode into two phonons and three phonons in InGaN films.

The solid curves in Fig. 2 are the calculated A_1(LO) and E_2(high) phonon frequencies with temperature using ω_0, M_1, and M_2 as fitting parameters (listed in Table 1). The other parameters for InGaN are obtained by linear interpolation method from those of InN and GaN. The agreement between the theoretical fit and experimental data is quite good. According to the calculations, the dominant contribution comes from the anharmonic coupling to other phonons through the three-phonon and four-phonon processes, especially in the high-temperature range, for five InGaN samples. In contrast, $\Delta\omega_s(T)$ makes minor contribution to the Raman shift. Moreover, in addition to a blueshift in the Raman frequency of InGaN compared with that of InN [9, 21], we note that the variation of ω_0 with Ga composition can be attributed well to the change of the lattice constant. Due to the incorporation of Ga substitutionally on the In sublattice, the lattice constant decreases linearly with the increase in the Ga composition [5], resulting in the increase of ω_0. It should also be noted that there are the apparent discrepancy between theory and experiment in

Table 1 The best fitting parameters for Raman frequencies [Eqs. (1) and (2)] and linewidths [Eq. (3)] of the A_1(LO), and E_2(high) modes in InGaN.

Raman modes	$In_{1-x}Ga_xN$	ω_0 (cm^{-1})	M_1 (cm^{-1})	M_2 (cm^{-1})	Γ_0 (cm^{-1})	N_1 (cm^{-1})	N_2 (cm^{-1})
A_1(LO)	0.06	591.3	−0.73	−0.45	90.2	5.25	3.13
	0.17	600.6	−0.89	−0.50	100.7	5.99	3.15
	0.30	617.2	−1.20	−0.61	130.5	6.82	3.55
	0.39	641.2	−1.46	−0.71	161.0	7.79	3.65
	0.91	730.6	−2.63	−0.12	40.3	16.98	0.90
E_2(high)	0.06	517.2	−0.20	−1.82	75.1	0.15	1.39
	0.17	524.8	−0.48	−1.61	81.8	0.41	1.34
	0.30	537.5	−0.89	−1.55	90.0	0.66	1.25
	0.39	561.0	−1.10	−1.40	93.4	1.01	1.21
	0.91	566.9	−2.59	−0.24	44.5	8.66	0.80

© 2012 WILEY-VCH Verlag GmbH & Co. KGaA, Weinheim

Fig. 2(b) for the cases of $x = 0.06$ and 0.17, which may be derived from the simply symmetric decay in Eq. (2) for E_2(high) mode.

The phonon broadening $\Gamma(T)$ mainly arises from inhomogeneous impurity phonon scattering and anharmonic decay. In analogy to the temperature dependence of Raman shift, the phonon broadening can be described with frequency ω_1 and ω_2 and the symmetric decay into three phonons [16–18]:

$$\Gamma(T) = \Gamma_0 + N_1[1 + n(T,\omega_1) + n(T,\omega_2)] + N_2\left[1 + 3n(T,\omega_0/3) + 3n^2(T,\omega_0/3)\right], \quad (3)$$

where Γ_0 denotes a damping contribution due to inherent defect or impurity scattering. The second term displays the asymmetric decay of three-phonon process, while the third term is the corresponding symmetric decay of the four-phonon process. Anharmonic constants of N_1 and N_2 are the relative probability of the decay into either two or three phonons, respectively. Figure 3 shows the least-squares fit of Eq. (3) (solid curves) for the temperature-dependent linewidths of the A_1(LO) and E_2(high) modes in InGaN. The fitting parameters Γ_0, N_1, and N_2 have also been given in Table 1. It can be clearly seen that Γ_0 of A_1(LO) and E_2(high) modes in $In_{1-x}Ga_xN$ firstly experience a rapid increasing depending on Ga composition ($x < 0.6$) due to the breakdown of the wave vector selection rules leading to participation of phonons with large wave vectors, then appear to decrease with Ga composition ($x > 0.6$), which can be attributed to the probability of the fluctuations in atom distribution of $In_{1-x}Ga_xN$ alloys [21]. On the other hand, the linewidth E_2(high) mode increase much more slowly with Ga composition than that of A_1(LO) mode, which possibly indicates that there are more channels for the decay of the A_1(LO) mode than for the decay of the E_2(high) mode in InGaN.

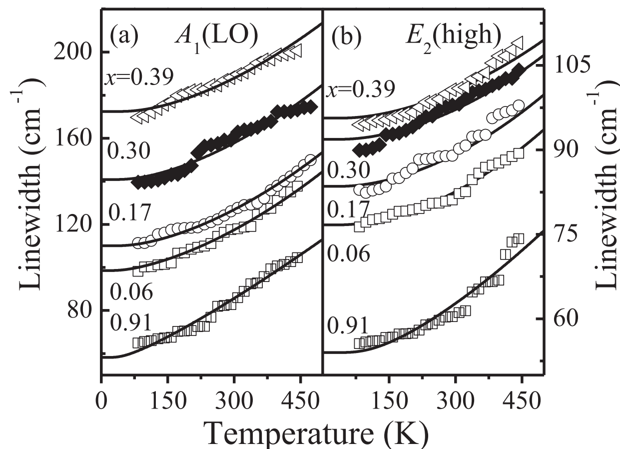

Figure 3 Temperature-dependent Raman linewidths of (a) A_1(LO) and (b) E_2(high) modes in InGaN with different Ga compositions. The solid curves are the theoretical calculation results with Eq. (3).

Figures 4(a) and (b) display the relative contributions (ratios of M_1/M_2 and N_1/N_2) of the three- and four-phonon processes to the total phonon decay for A_1(LO) and E_2(high) modes. The variation of N_1/N_2 is very close to that of M_1/M_2, confirming the reliability of our results obtained from the theoretical fitting. For InN, the four-phonon process makes minor contribution in the anharmonic coupling of the A_1(LO) modes. In contrast, the E_2(high) phonon of InN can only decay into three phonons [17, 25]. With increasing Ga composition, the ratios of M_1/M_2 and N_1/N_2 rapidly increase for two modes in InGaN, revealing the increasing contribution of the three-phonon process over the four-phonon one. The change of M_1/M_2 and N_1/N_2 is consistent with the fluctuation in phonon DOS due to the increase Ga composition. The incorporation of Ga in InN causes lattice defect and structural disorder, which break down the translational symmetry of InN. As a consequence, not only the Brillouin zone-center phonons but also the phonons at Brillouin zone-edges have contribution to the first-order Raman scattering.

By the aid of the calculated DOS of InN [26] and GaN [27] shown in Fig. 4(c), we have attempted to give a qualitative interpretation about the changes of the ratios of M_1/M_2 and N_1/N_2 with the Ga composition. For the A_1(LO) mode, the increase of ω_0 in InGaN causes large values of ω_1 and ω_2, resulting in the fast increase of the contribution of the three-phonon process, whereas the blueshift of $\omega_0/3$ ($\sim$200 cm^{-1}) leads to a decrease in the probability of the four-phonon process; for the E_2(high) mode, the increase of ω_0 with Ga composition leads to a decrease of the phonon DOS in InGaN at $\omega_0/3$ ($\sim$170 cm^{-1}) due to the significant decrease of InN phonon DOS there, *i.e.*, the reduction of the four-phonon process contribution. Therefore, as shown in Fig. 4(a) and (b), the values of M_1/M_2 and N_1/N_2 in InGaN are larger than those of InN. The above results demonstrate unambiguously that with the increase of Ga composition in InGaN the three-phonon process gradually enhances the anharmonic shift and broadening of the A_1(LO) and E_2(high) modes, though the four-phonon process is adequately responsible for the anharmonic decay process.

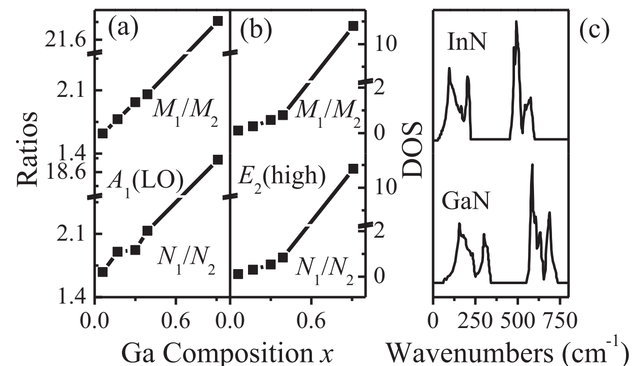

Figure 4 Ga-composition dependence of ratios M_1/M_2 and N_1/N_2 for (a) A_1(LO) and (b) E_2(high) modes in InGaN. (c) Calculated phonon DOS of InN (from Ref. [18]) and GaN (from Ref. [19]).

© 2012 WILEY-VCH Verlag GmbH & Co. KGaA, Weinheim

4 Conclusions In summary, detailed Raman spectra of $In_{1-x}Ga_xN$ ($0.06 \leq \chi \leq 0.91$) thin films grown by reactive radio-frequency magnetron sputtering on sapphire substrates have been investigated in the temperature range of 83–443 K by Lorentz fitting, with the emphasis on the A_1(LO), and E_2(high) modes. By the aid of a model involving the contributions of the thermal expansion, lattice-mismatch-induced strain, as well as three- and four-phonon coupling, we have clearly illustrated the temperature effect on the phonon frequency and linewidth of InGaN. We have demonstrated that with increasing Ga composition the contribution of the three-phonon process increases while that of four-phonon process reduces, due to the variation of structural properties and phonon DOS in InGaN. The phonon properties provide an experimental basis for further theoretical investigation and the design of InGaN-based devices.

Acknowledgements This work was supported by the special fund of training outstanding young teachers of shanghai university under contract yyy10045.

References

[1] X. Zhang, X. Wang, H. Xiao, C. Yang, J. Ran, C. Wang, Q. Hou, and J. Li, J. Phys. D **40**, 7335 (2007).
[2] O. Jani, I. Ferguson, C. Honsberg, and S. Kurtz, Appl. Phys. Lett. **91**, 132117 (2007).
[3] C. Neufeld, N. Toledo, S. Cruz, M. Iza, S. Denbaara, and U. Mishra, Appl. Phys. Lett. **91**, 132117 (2007).
[4] X. Zheng, R. Horng, D. Wuu, M. Chu, W. Liao, M. Wu, R. Lin, and Y. Lu, Appl. Phys. Lett. **93**, 261108 (2008).
[5] G. Q. Xin, Y. Kusunoki, Y. L. Ding, T. Tanaka, and M. Nishio, J. Appl. Phys. **49**, 081203 (2010).
[6] G. B. Stringfellow, J. Cryst. Growth **312**, 735 (2010).
[7] W. Walukiewicz, J. W. Ager, III, K. M. Yu, Z. Liliental-Weber, J. Wu, S. X. Li, R. E. Jones, and J. D. Denlinger, J. Phys. D, Appl. Phys. **39**, R83 (2006).
[8] J. Wu, J. Appl. Phys. **106**, 011101 (2009).
[9] R. Oliva and J. Ibáñez, R. Cuscó, R. Kudrawiec, J. Serafinczuk, O. Martínez, J. Jiménez, M. Henini, C. Boney, A. Bensaoula, and L. Artú